Nash Game Based Distributed Control Design for Balancing of Traffic Density over Freeway Networks

Dominik Pisarski, Carlos Canudas de Wit

Nash Game Based Distributed Control Design for Balancing of Traffic Density over Freeway Networks

Dominik Pisarski and Carlos Canudas de Wit

***Abstract*—In this paper, we study the problem of optimal balancing of vehicle density in the freeway traffic. The optimization is performed in a distributed manner by utilizing the controllability properties of the freeway network represented by the Cell Transmission Model. By using these properties, we identify the subsystems to be controlled by local ramp meters. The optimization problem is then formulated as a non-cooperative Nash game that is solved by decomposing it into a set of two-players hierarchical and competitive games. The process of optimization employs the communication channels matching the switching structure of system interconnectivity. By defining the internal model for the boundary flows, local optimal control problems are efficiently solved by utilizing the method of Linear Quadratic Regulator. The developed control strategy is tested via numerical simulations in two scenarios for uniformly congested and transient traffic.**

I. Introduction

Freeway traffic management is nowadays one of the most important factors impacting on economics, environment and the quality of our daily life. A wide range of specialized sensing, ramp metering and variable speed limiting instrumentation is already in use, performing optimal control policies that result in shortened travel delays, reduced pollution, decreased number of accidents and many other benefits.

A common objective for freeway system regulation and control is to decrease the time of travel incurred by all drivers while maximizing the traffic flow [1], [2]. For this purpose, the relevant metrics like Total Travel Spent, Total Travel Distance and Total Input Volume were introduced. In the process of optimization, they are combined with some additional terms that penalize abrupt variations in ramp metering and speed limiting signals [3]. General objectives such as congestion, pollution, and energy reduction are also in order.

Most of the optimal freeway controllers are implemented through the centralized architectures [4]. The optimization methods used in such architecture suffer from a lack of scalability. The computational time increases exponentially with the size of the system, and thus the tractable length of freeway is usually limited to several kilometers. Moreover, the centralized optimization solvers require permanent and complete state information and this may not be attainable due to numerous package loses. These issues are faced by implementing distributed optimization methods. A dual decomposition method was proposed in [5] to control the traffic flow in the airspace system. Distributed controller's architecture in freeway traffic flow control was investigated in [6], where the authors isolated freeway clusters and defined collaborative mechanisms to achieve a desired performance of the overall system. Distributed and centralized model predictive control schemes for freeway traffic control were compared in [7]. The authors demonstrated that a distributed controller exhibits the performance comparable with a centralized one, and it is less sensitive to model uncertainties. In this paper, based on the Nash game formulation, we will design a distributed optimal controller to regulate freeway traffic flow. The major contributions lie within the modularity of the controller's structure and the establishment of the dynamically adapting system division allowing for proper formulation and effective solution of the distributed game problem.

The control objective will be to balance traffic density. This balancing can be perceived as equalizing the average inter-distance between vehicles which is eligible for smooth and safety ecodriving. Naturally emerging question is for the level of the balanced density that provides also effective flow of the traffic volume. In our setting, we will tend to balance the traffic density at the level that reduces the Total Travel Spent. We will also investigate the impact of density balancing on the propagation of shock waves. For our previous studies on the traffic state balancing in the context of the equilibrium sets, the reader is referred to the papers [10], [11].

For distributed controller, we will impose the following requirements: functional symmetry in the controller's structure, the minimum computational time and information exchange for the optimization process. The symmetry will be achieved by splitting the controller into modules realizing the same computational procedures. Modular type of architecture is convenient for system assembling and maintenance. Each of the modules will compute its optimal decision by using local traffic state and some supplementary information arriving from other controllers. To perform the optimization under the proposed distributed architecture, the optimal control problem will be formulated as a Nash game, where each player (controller) will optimize its local subsystem with respect to decisions of the other players.

A Nash game based approach for freeway traffic optimization was reported in [8]. The authors utilized the mechanism of the distributed predictive control based on game theory (GT-DMPC, introduced in [9]) pointing on computational complexity and slow convergence of the optimization procedure

Dominik Pisarski is with NeCS team INRIA Rhone-Alpes, Grenoble, France, *dominik.pisarski@inria.fr*

C. Canudas-de-Wit is a director of reearch at the CNRS, GIPSA-Lab. NeCS team, Grenoble, France, *carlos.canudas-de-wit@gipsa-lab.grenoble-inp.fr*

when applied to a large scale traffic network. The convergence problem may result from an arbitrary and static system division assumed by the authors. As we will demonstrate, in the case of an arbitrary system division, there is a risk of loss of controllability, and therefore the uniqueness of the optimal solution. We will also show that, due to the presence of the switched interfacing flows, it is forbidden to split a freeway system in an arbitrary manner. In contrast to [8], we will design a dynamical partitioning scheme that will be adapting the local subsystems according to the actual traffic state such to provide the controllability of the inputs involved in the game problem. The controllability analysis will also allow us to decompose the overall game problem and solve it by performing a sequence of simple two-player games.

II. The Cell-Transmission Model of Freeway Traffic

Most of the freeway traffic models are based on the scalar vehicle conservation law. For a space interval $[a, b]$ at each time instant t the rate of change of number of vehicles is equal to the difference in flows at the endpoints a and b, i.e.:

$$\frac{\mathrm{d}}{\mathrm{d}t}\int_a^b \rho(y,t)\,\mathrm{d}y = \phi(a,t) - \phi(b,t)\,. \tag{1}$$

Here $\rho(y,t)$ and $\phi(y,t)$ stands for the space-time distributions of vehicle density and flow, respectively. In general, the density-flow relation is nonlinear, and therefore the relevant numerical methods for solving (1) need to be applied.

In this paper, we utilize the Cell-Transmission Model [12]. The model can be perceived as the Godunov's [13] difference scheme for (1) under the assumption that the density-flow relation, called the fundamental diagram, is given in a triangular form. A freeway is represented as a sequence of n cells as demonstrated in Fig. 1. Each cell is assumed to have at most one on-ramp and one off-ramp. The total number of on-ramps is m. We adopt the following notation: ρ – vehicle density, l – queue length, ϕ – mainstream flow, r – on-ramp flow, s – off-ramp flow, $\bar{\beta}$ – split ratio, u – controlled on-ramp demand, $\hat{D}$ – external on-ramp demand, $\bar{D}$ – boundary demand, $\bar{S}$ – boundary supply, v – free flow velocity, w – congestion wave speed, F – mainstream flow capacity, ρ^{cr} – critical density ($\rho^{cr} = F/v$), $\bar{\rho}$ – jam density, $\bar{l}$ – on-ramp storage capacity, L – cell length. Throughout this paper, we assume the same number of lanes for each cell.

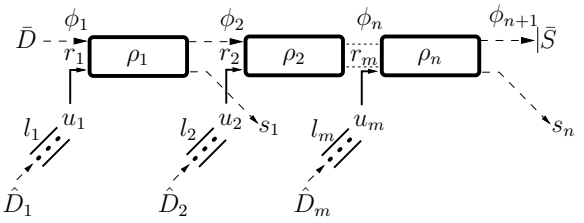

Figure 1. Freeway divided into n cells. Each cell can be accompanied with at most one on-ramp and one off-ramp.

Let $i = 1, 2, ..., n$ and $j = 1, 2, ..., m$ be the index for the cells and on-ramps, respectively. We associate each on-ramp flow r_j to the cell i according to a freeway architecture. Then, the evolution of the Cell-Transmission Model is described by the following difference equations:

$$\begin{aligned} \rho_i(k+1) &= \rho_i(k) + \frac{\Delta t}{L_i}\left[\phi_i(k) + r_j(k) - \phi_{i+1}(k) - s_i(k)\right]\,, \\ l_j(k+1) &= l_j(k) + \Delta t\left[\hat{D}_j(k) - r_j(k)\right]\,. \end{aligned} \tag{2}$$

where the initial state $\rho(k=0), l(k=0)$ is given. Time step Δt between instants k and $k+1$ must fulfil the Courant-Friedrichs-Lewy stability condition (for details see [14]).

Throughout this paper, we use Daganzo's Priority Merge Model [15]. The model introduces the so called merging parameter $p \in [0, 1]$. It captures the priorities between mainstream flow ϕ and on-ramp flow r when merging in a section under highly congested states. In order to determine the value of the merging parameter p, one should consider geometric properties of on-ramp as well as drivers' behavior.

Let us introduce Demand D_i and Supply S_i functions:

$$\begin{aligned} D_i(k) &= \min\left\{\bar{\beta}_i v_i \rho_i(k), F_i\right\}\,, \\ S_i(k) &= \min\left\{w_i(\bar{\rho}_i - \rho_i(k)), F_i\right\}\,, \end{aligned} \tag{3}$$

Here the parameter $\bar{\beta}_i \in (0, 1]$ is the split ratio defined as $\bar{\beta}_i = \phi_{i+1}/(\phi_{i+1} + s_i)$. By using (3) the mainstream and on-ramp flows are computed as follows:

$$\begin{aligned} &\text{if } D_{i-1}(k) + u_j(k) \le S_i(k)\ : \\ &\phi_i(k) = D_{i-1}(k)\,, \\ &r_j(k) = u_j(k) \\ &\text{otherwise}\ : \\ &\phi_i(k) = \operatorname{mid}\left\{D_{i-1}(k), S_i(k) - u_j(k), (1-p_j)\,S_i(k)\right\}\,, \\ &r_i(k) = \operatorname{mid}\left\{u_j(k), S_i(k) - D_{i-1}(k), p_j\,S_i(k)\right\}\,. \end{aligned} \tag{4}$$

Here the function $\operatorname{mid}\{\cdot\}$ returns the middle value, i.e.: $\operatorname{mid}\{a, b, c\} = a$ if $b \le a \le c$ or $c \le a \le b$. For the off-ramp flows we assume:

$$s_i(k) = \frac{1 - \bar{\beta}_i}{\bar{\beta}_i}\,\phi_{i+1}(k)\,. \tag{5}$$

Throughout this paper, a cell i will be said to be in the free flow state if $\rho_i \le \rho_i^{cr}$. Otherwise, it will be said to be in the congested state.

For convenience of the further studies we will rewrite the governing equation of CTM in a compact form. By introducing the state vector:

$$x = [\ \overbrace{\rho_1, \rho_2, ..., \rho_n}^{\text{CTM densities}}\ ,\ \overbrace{l_1, l_2, ..., l_m}^{\text{on-ramp queues}}\ ]^{\intercal} \tag{6}$$

and assuming the following controlled input vector:

$$u = [\ \overbrace{u_1, u_2, ..., u_m}^{\text{on-ramp demands}}\ ]^{\intercal} \tag{7}$$

we can represent the governing equation (2) in the form of a switched system:

$$\begin{aligned} &x(k+1) = x(k) + \Delta t\left(A_{s(k)}\,x(k) + B_{s(k)}\,u(k) + C_{s(k)}(k)\right)\,, \\ &s(k) = f(x(k), u(k))\,. \end{aligned} \tag{8}$$

The variable s switches the system mode according to the laws given in (3) and (4). The boundary conditions $\bar{D}(k)$, $\bar{S}(k)$, $\hat{D}_1(k), \hat{D}_2(k), ..., \hat{D}_m(k)$ appear in the vector C_s. An illustrative example on how to build up A, B and C can be found in [10].

The state space $\mathcal{X} \subset \mathcal{R}^{n+m}$ is non-negative and it is upper bounded by the storage capacities of the mainstream and on-ramp lanes, i.e. for the states representing vehicle densities the bound is equal to the jam density $\bar{\rho}$ while the states corresponding to the queue lengths must not exceed the storage capacities of the on-ramps $\bar{l}$:

$$\begin{aligned} &0 \leq x_i \leq \bar{\rho}\,,\ i = 1, 2, ..., n\,, \\ &0 \leq x_i \leq \bar{l}_j\,,\ i = n+1, n+2, ..., n+m\,,\ j = i-n\,. \end{aligned} \tag{9}$$

To determine the set of the admissible controls $\mathcal{U} \subset \mathcal{R}^m$, we need to take a closer look on its physical constraints. The on-ramp vehicle flow in only one direction, and thus the controlled on-ramp demand must not be negative. For the upper bound, the requirement is that the controlled demand at each time step can not exceed the so called virtual demand that equals to the sum of the external on-ramp demand and the flow produced by the queueing vehicles (see [16]):

$$0 \leq u_j \leq \hat{D}_j + \frac{1}{\Delta t} l_j\,,\ j = 1, 2, ..., m\,. \tag{10}$$

III. Controllability of the freeway links

In this section, we recall the fundamental facts on the controllability of the freeway state. These facts will later determine the scheme for system partitioning and the methodology for solving distributed game problem.

Let us first introduce the notion of the freeway links. By a link we will mean any freeway section, composed of a group of cells, that is separated by two successive on-ramps. Throughout this paper, we will consider only four types of the links, each with different state structure. The first two types of the links consist of the cells being in the same mode, free flow (F) or congested (C), as depicted in Fig. 2. These links will be referred later as the homogeneous state links. The remaining

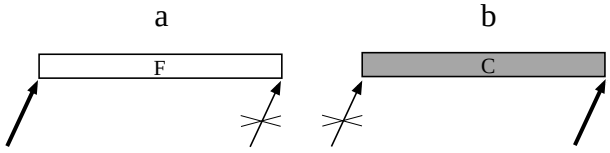

Figure 2. Homogeneous state links under their control inputs. The links are controllable by the inputs denoted by the bold arrows.

two types of the links, referred as the mixed state links, will be composed of the cells of both modes, assuming that the state is structured according to the two cases presented in Fig. 3. More complex internal state structures are very rarely observed through the real traffic data.

To verify the controllability of the considered links, let us rewrite the vehicle conservation law (1) in the form of a partial differential equation. We assume here that for every freeway position at every time instant the flow can be represented as

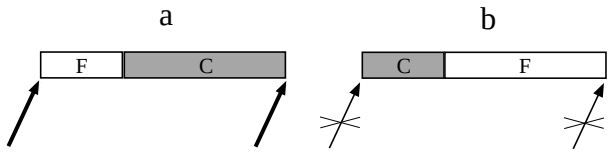

Figure 3. Mixed state links under their control inputs. The links are controllable by the inputs denoted by the bold arrows.

a function of vehicle density, i.e. : $\phi(y,t) = \phi(\rho(y,t))$. Then, (1) can be written as follows:

$$\frac{\partial \rho}{\partial t} + \phi'(\rho)\frac{\partial \rho}{\partial y} = 0\,. \tag{11}$$

Depending on the internal state of the link, we can have either $\phi'(\rho) > 0$ (for a section in the free flow state) or $\phi'(\rho) < 0$ (for a section in the congested state). Respecting the fundamental diagram (given by: $\phi(\rho) = v\rho$ if $\rho \leq \rho^{cr}$, and $\phi(\rho) = w(\bar{\rho} - \rho)$ otherwise), for a section in the free flow state we have $\phi'(\rho) = v$. Similarly, for the congested section $\phi'(\rho) = -w$. Now suppose we are given the initial condition $\rho(y, 0)$. Then, the solution to (11) is represented as follows:

$$\begin{aligned} &\rho(y,t) = \rho(y - vt, 0) \quad \text{for free flow state section}\,, \\ &\rho(y,t) = \rho(y + wt, 0) \quad \text{for congested state section}\,. \end{aligned} \tag{12}$$

The solution (12) represents the wave propagating downstream or upstream under the free flow or the congested state, respectively. As a consequence, in order to control a link in the free flow state, we need to place a controller at the upstream bound (Fig. 2a). For a congested link, a controller is supposed to be located at the downstream bound (Fig. 2b). In the case of the link containing successively located free flow and congested section (Fig. 3a), the state dynamics is under control of both inputs. In the situation with the reverse state (Fig. 3b), a link stays uncontrollable.

The controllability results presented here are also valid for a wide class of discrete representations of the conservation law. For the Cell Transmission Model, the analogous results may be easily verified by means of the controllability matrix.

IV. System partitioning and state information pattern

In the section V, we will pose a Nash problem, where each of the control input will tend to optimize its local subsystem. Here, we will establish a method for selection of these subsystems by defining an input-state assignment. We assume that each of the inputs receives a full state information of the two surrounding links as demonstrated in Fig. 4.

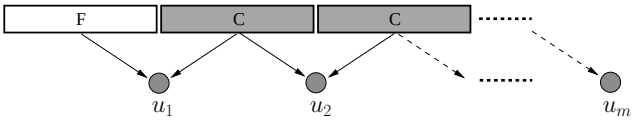

Figure 4. State information pattern. Each of the controllers receives the density information of two neighbouring links.

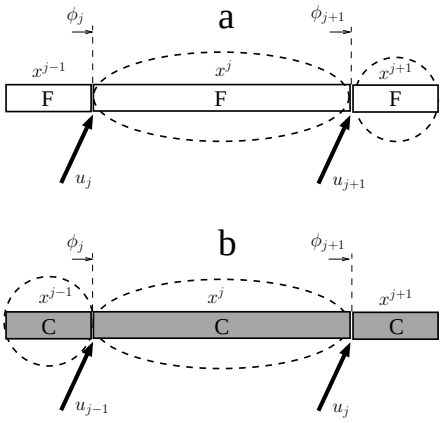

Figure 5. System partitioning in the cases of the homogeneous free flow state link (a) and the congested state link (b).

Let us define x^j as a part of the state vector x that is assigned to the input u_j:

$$x^j = \left[\rho_1^j, \rho_2^j, ..., \rho_{n_j}^j, l_j\right]^\mathsf{T} . \tag{13}$$

The assignment of the subsystem x^j to u_j is made based on the following rule: x^j is composed of the cells of the closest downstream/upstream link for u_j, if it is in the free flow/congested state. The assignment in the case of the homogeneous state links is presented in Fig. 5a,b. The total number of cells assigned to the input u_j is denoted by n_j. Note that besides the controllability of x^j, the assumed partitioning provides that:

Each of the boundary flows for the link x_j is uniquely determined by only one subsystem (x_j or its neighbour). (The statement will be later refereed as the separation principle). Indeed, in the free flow case, we have $\phi_j = D(x^{j-1})$, $\phi_{j+1} = D(x^j)$. For the congested case, we have $\phi_j = S(x^j)$, $\phi_{j+1} = S(x^{j+1})$ (Here the notation $D(x^j)$ and $S(x^j)$ stands for the demand and the supply corresponding to the link x^j). The uniqueness of the boundary condition is crucial for setting the distributed game problem. We will be able to decouple the dynamics of the subsystems and solve the local optimization problems, where the controllers will optimize their subsystems with respect to given boundary conditions.

In the case of the mixed state links, the separation principle results in the subsystem selection as depicted in Fig. 6. Note that ϕ_{j+1} may be switched between demand of the free flow section and supply of the congested section according to the model of the interfacing flow: $\phi_{j+1} = \min\{D(x^j), S(x^{j+1})\}$. In this case, the dynamics for these sections must be solved jointly. The subsystem selection for the mixed state links will be denoted by $x^{j,\,j+1}$ and will be meant to be optimized by both inputs u_j and u_{j+1}. The presence of switching interfacing flows follows the statement that the structure of system division can not be fixed.

We will now give the explicit dynamical representations of the subsystems discussed above. We assume that inside each of the links, the cell parameters v, w and $\bar{\rho}$ are equal. We also assume that in each of the links, there is only one off-ramp (with associated split ratio $\bar{\beta}_j$), and it is placed in

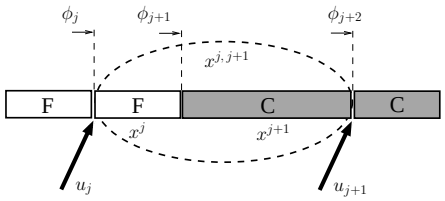

Figure 6. System partitioning in the case of the mixed state link.

the last cell of the link. This assumption will later become significant for the method of solving optimal control problem, where we will use an autonomous form of the dynamical equations. Note that this assumption meets most of the existing freeway architectures, where off-ramps are located just before on-ramps. By introducing the inverted cell lengths matrix: $L_{inv}^j = \text{diag}\,(1/L_1^j, 1/L_2^j, ..., 1/L_{n_j}^j, 1)$ and the matrices:

$$\begin{aligned} A_f &= v_j L_{inv}^j \begin{bmatrix} -1 & & & & 0 \\ 1 & -1 & & & 0 \\ & \ddots & \ddots & & \vdots \\ & & 1 & -1 & 0 \\ 0 & \cdots & 0 & 0 & 0 \end{bmatrix}, \\ B_f &= L_{inv}^j \begin{bmatrix} 1 \\ 0 \\ \vdots \\ 0 \\ -1 \end{bmatrix}, \; C_f = L_{inv}^j \begin{bmatrix} 1 \\ 0 \\ \vdots \\ 0 \\ 0 \end{bmatrix}, \; D_f = L_{inv}^j \begin{bmatrix} 0 \\ 0 \\ \vdots \\ 0 \\ 1 \end{bmatrix}, \end{aligned} \tag{14}$$

the dynamical equation of the free flow state link is represented by:

$$\begin{aligned} x^j(k+1) = x^j(k) + \Delta t(&A_f x^j(k) + B_f u_j(k) + \\ &+ C_f \bar{D}_j(k) + D_f \hat{D}_j(k)) . \end{aligned} \tag{15}$$

Here by $\bar{D}_j(k)$ we will denote the mainstream demand for the link j. Note that according to the assumed merging model (4), the system (15) is valid only if:

$$u_j(k) \le F_j - \bar{D}_j(k) \;\; \text{for all} \;\; k\,, \tag{16}$$

where F_j stands for the flow capacity of the link j. Similarly, by introducing:

$$\begin{aligned} A_c &= w_j\, L_{inv}^j \begin{bmatrix} -1 & 1 & & & 0 \\ & -1 & 1 & & 0 \\ & & \ddots & \ddots & \vdots \\ & & & -1 & 0 \\ 0 & \cdots & 0 & 0 & 0 \end{bmatrix}, \\ B_c &= L_{inv}^j \begin{bmatrix} 0 \\ 0 \\ \vdots \\ \frac{1}{\bar{\beta}_j} \\ -1 \end{bmatrix}, \; C_c = L_{inv}^j \begin{bmatrix} 0 \\ 0 \\ \vdots \\ 1 \\ 0 \end{bmatrix}, \; D_c = L_{inv}^j \begin{bmatrix} 0 \\ 0 \\ \vdots \\ 0 \\ 1 \end{bmatrix}, \end{aligned} \tag{17}$$

the dynamics of the congested state link is governed by:

$$x^j(k+1) = x^j(k) + \Delta t(A_c x^j(k) + B_c u_j(k) + \\ + C_c(w_j\bar{\rho}_j - \frac{1}{\bar{\beta}_j}\bar{S}_j(k)) + D_c\hat{D}_j(k))\,, \tag{18}$$

where $\bar{S}_j(k)$ stands for the mainstream supply for the link j. Respecting the merging model (4) the system (18) is valid under the condition:

$$u_j(k) \leq p\,\bar{S}_j(k) \quad \text{for all } \; k\,. \tag{19}$$

Here $p\,\bar{S}_j$ is the supply available for the on-ramp demand. To write down the dynamical equation of the controllable mixed state link, we introduce the following matrices:

$$A_{fc}(k) = \begin{bmatrix} A_f(k) & \\ & A_c(k) \end{bmatrix}, B'_f = \begin{bmatrix} B_f \\ 0 \end{bmatrix}, C'_f = \begin{bmatrix} C_f \\ 0 \end{bmatrix}, \\ D'_f = \begin{bmatrix} D_f \\ 0 \end{bmatrix}, B'_c = \begin{bmatrix} 0 \\ B_c \end{bmatrix}, C'_c = \begin{bmatrix} 0 \\ C_c \end{bmatrix}, D'_c = \begin{bmatrix} 0 \\ D_c \end{bmatrix}. \tag{20}$$

Here the system matrix A_{fc} is composed of the switching matrices $A_f(k)$ and $A_c(k)$ preserving the structures of A_f and A_c except for the rows corresponding to the interfacing flow $\phi_{j+1}(k) = \min\{D(x^j(k)), S(x^{j+1}(k))\}$. The sizes of $A_f(k)$ and $A_c(k)$ are being adjusted according to the position of the congestion wave. The controlled mixed state links are governed by the following dynamical equation:

$$x^{j,\,j+1}(k+1) = x^{j,\,j+1}(k) + \Delta t\, A_{fc}(k)x^{j,\,j+1}(k) + \\ + \Delta t\left(B'_f u_j(k) + C'_f\bar{D}_j(k) + D'_f\hat{D}_j(k)\right) + \\ + \Delta t\left(B'_c u_{j+1}(k) + C'_c(w_j\bar{\rho}_j - \bar{S}_{j+1}(k)) + D'_c\hat{D}_{j+1}(k)\right). \tag{21}$$

For (21), we assume:

$$u_j(k) \leq F_j - D_j(k)\,, \quad u_{j+1}(k) \leq p\,S_{j+1}(k) \quad \text{for all } \; k\,. \tag{22}$$

The uncontrollable links, as depicted in Fig. 3b, evolve according to the following dynamics:

$$x(k+1) = x(k) + \Delta t\, A_{cf}(k)x(k)\,, \tag{23}$$

with the switching matrix $A_{cf} = \text{diag}(A_c(k), A_f(k))$.

V. Optimization Problem

A freeway partitioned according to the scheme presented in the previous section is now ready for optimization. The goal is to formulate an optimal control problem that can be solved by following the state information pattern presented in the previous section. For the solution procedure, we allow that each of the controllers communicates under the topology presented in Fig. 7a. As it will be found later, this topology captures all information channels involved during the solution for different state combinations 7b–d. The optimization problem will be formulated as a non-cooperative game.

For each of the controllable inputs u_j (referred later also as the players), we define local objective function $J_j(u_j, x^j)$ that explicitly depends on the control u_j and its assigned the state vector x^j. Note that x^j may be also influenced by some

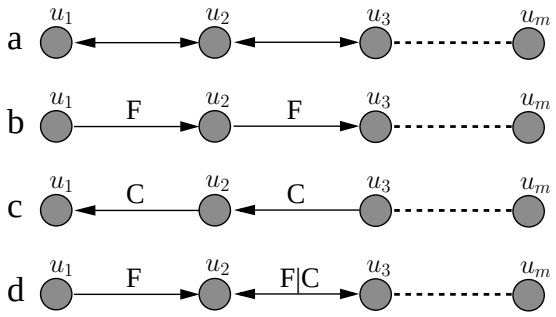

Figure 7. Channels used for information exchange during the optimization process. The general topology (a), channels used for different state combinations (b)–(d).

of the other controllers through the boundary conditions (this will be specified in the following section). Let u_{-j} be the set of the decision of the controllers that may influence the state x^j, excluding the decision of u_j. The objective function can be now represented by $J_j(u_j, u_{-j})$. Throughout this paper, we consider the optimization problem stated as the following non-cooperative game:

Problem 1 *(non-cooperative Nash game)*

$$\text{Find } \; \{u_j^*\} \text{ such that } \forall j: \; u_j^* = \text{argmin}\, J_j(u_j, u_{-j}^*)\,.$$

The set of decisions $\{u_j^*\}$ is called the Nash Equilibrium and this is the strategy such that no unilateral deviation in decision by any single player is profitable for that player. For extensive studies on the Nash equilibrium solution concept a reader is refereed to [17]. To guarantee that the Nash equilibrium exists, every objective function J_j needs to be continuous in all its arguments and strictly convex in u_j. Both conditions will be fulfilled in our setting.

Observe that in general, to solve the Problem 1, each of the players requires information of the decisions of all other players that may affect its objective function. We will demonstrate that, for the freeway traffic, the problem of finding the Nash Equilibrium can be solved under the communication channels represented by the graph shown in Fig. 7a. The key is that the identical line graph represents system interconnectivity for CTM. In that case of CTM, the arrows would indicate the directions in which a decision propagates affecting the system. Now assume that a subsystem j is affected by more than one decision from each of the directions. For example, let $u_{-j} = \{u_{j-2}, u_{j-1}, u_{j+1}, u_{j+2}\}$. In practice, for a subsystem j, the decisions u_{j-2} and u_{j-1} will be embedded into its upstream boundary flow. Similarly, u_{j+1} and u_{j+2} will be embedded into j's downstream boundary flow. Thus, to solve the game problem, there is no need to transfer all optimal decisions, but instead the neighbouring controllers will exchange their optimal demand/supply informations. The Problem 1 then will be decomposed and solved by performing a sequence of two-player games. The games will be either hierarchical or competitive depending on the state (homogeneous or mixed) inside the link between the players. Each of these games will be executed by solving the local optimal control problems discussed in the section VI.

A. Non-Cooperative Game for the homogeneous state links

Let us consider the homogeneous state links in the free flow and the congested state as depicted in Fig. 8a and Fig. 8b, respectively. A decision taken by any of the inputs propagates in accordance to the direction of travel of traffic wave (downstream for the free flow state case and upstream for the congested state case). It therefore follows that for the homogeneous state links, among two of the neighbouring inputs there is only one that can affect the state of the other. The Nash game for such pair of inputs has the controllability imposed hierarchy. This sort of game is referred as hierarchical or the Stackelberg game. The local objective functions takes

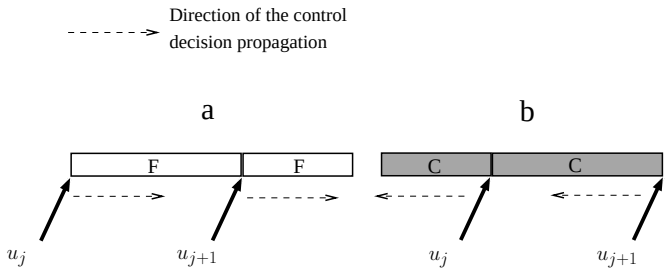

Figure 8. Propagation of the control decisions in the case of the homogeneous state links.

the following forms:

$$J_j(u_j, x^j(u_j))\,,\;\; J_{j+1}(u_{j+1}, x^{j+1}(u_j, u_{j+1})) \tag{24}$$

in the case of the free flow state links and:

$$J_j(u_j, x^j(u_j, u_{j+1}))\,,\;\; J_{j+1}(u_{j+1}, x^{j+1}(u_{j+1})) \tag{25}$$

in the case of the congested state links. In the sequel, we will use the explicit notations, i.e. $J_j(u_j)$ instead of $J_j(u_j, x^j(u_j))$ and $J_j(u_j, u_{j+1})$ instead of $J_j(u_j, x^j(u_j, u_{j+1}))$.

The Stackelberg game enables to reach the Nash Equilibrium by executing only one local optimization for each of the players. Formally, the Nash equilibrium for the Stackelberg two-player game in the free flow state case is written as follows:

$$u_j^* = \text{argmin}\, J_j(u_j)\,,\;\; u_{j+1}^* = \text{argmin}\, J_{j+1}(u_j^*, u_{j+1})\,. \tag{26}$$

Here the player j is the leader and player $j+1$ is the follower. Similarly, for the congested state case the Stackelberg game is:

$$u_j^* = \text{argmin}\, J_j(u_j, u_{j+1}^*)\,,\;\; u_{j+1}^* = \text{argmin}\, J_{j+1}(u_{j+1})\,, \tag{27}$$

with $j+1$ as the leader and j as the follower. The procedures to solve (26) and (27) are straightforward:

Procedure 1 *(free flow state links)*

Step 1 Find $u_j^* = \text{argmin}\, J_j(u_j)$,
Step 2 Find $u_{j+1}^* = \text{argmin}\, J_{j+1}(u_j^*, u_{j+1})$,

Procedure 2 *(congested state links)*

Step 1 Find $u_{j+1}^* = \text{argmin}\, J_{j+1}(u_{j+1})$,
Step 2 Find $u_j^* = \text{argmin}\, J_j(u_j, u_{j+1}^*)$,

B. Non-Cooperative Game for the mixed state links

Now we will consider the case of the mixed state link (see Fig. 9). Here, the two neighbouring inputs compete with each other in optimizing a dynamically coupled link. Decision of the player j may influence the value of objective function of the player $j+1$ and vice versa. The Nash Equilibrium for such

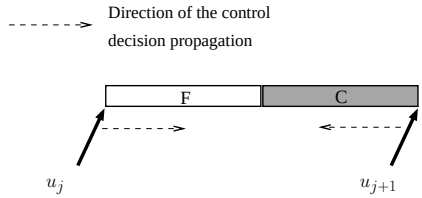

Figure 9. Propagation of the control decisions in the case of the mixed state links.

a game is written as follows:

$$u_j^* = \text{argmin}\, J_j(u_j, u_{j+1}^*)\,,\;\; u_{j+1}^* = \text{argmin}\, J_{j+1}(u_j^*, u_{j+1})\,. \tag{28}$$

We can solve (28) by executing the following procedure:

Procedure 3 *(mixed state links)*

Step 1 Initialize $u_j^* = u_{ini}$, assume ϵ_1, ϵ_2 as small positive numbers,
Step 2 Find $u_{j+1}^* = \text{argmin}\, J_{j+1}(u_j^*, u_{j+1})$,
Step 3 Find $u_j^* = \text{argmin}\, J_j(u_j, u_{j+1}^*)$,
Step 4 Repeat Steps 2, 3 until $\Delta\|J_j\| < \epsilon_1$, $\Delta\|J_{j+1}\| < \epsilon_2$ ($\Delta\|J_j\|$ stands for the incremental change of the norm of the objective function J_j).

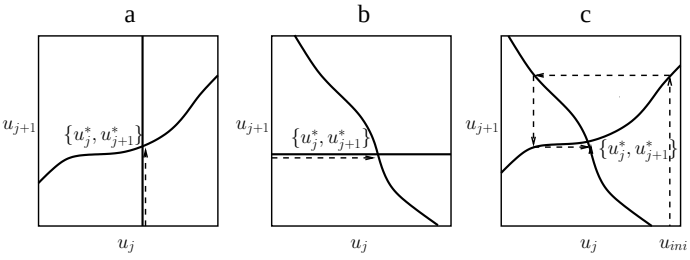

Figure 10. Best response curves and the Nash Equilibria. The arrows represent the procedure steps for finding the Nash Equilibria in the case of the free flow state Stackelberg game (a), the congested state Stackelberg game (b) and the mixed state competitive game (c).

Solution of both types of games can be visualized in simplified 2D representation. The curves depicted in Fig. 10a–c represent the best responses to the decision of the other player (the curves stretched along the horizontal lines stand for the best responses of the players u_{j+1} to the decisions of the players u_j). The crossing points of the curves represent the Nash Equilibria. The procedure steps for solving the games (a,b–Stackelberg games, c–competitive game) are executed as indicated by the arrows.

C. An Illustrative Example

Here we present an example on how the game is meant to be executed along several links of a freeway. We consider six

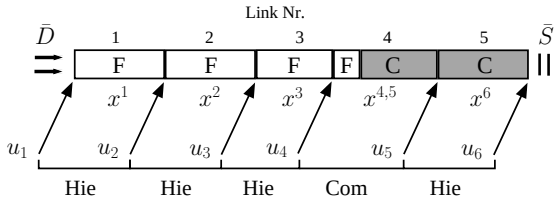

Figure 11. A section of a freeway used in the example of distributed search of the Nash equilibrium. *Hie* and *Com* stands for hierarchical and competitive game, respectively.

controlled on-ramps located as shown in Fig. 11. The first three upstream links are fully in the free flow state. The congestion begins inside the fourth link, and it stretches downstream the rest of a freeway. For such a state, the inputs u_1, u_2, u_3 and u_6 will optimize the links 1,2,3 and 5, respectively. The inputs u_4 and u_5 will compete for the link 4. The optimization process is performed through the following steps:

Procedure 4 *(illustrative example)*

Step 1 u_1 optimizes J_1 with respect to the given boundary demand $\bar{D}$. Next, u_1 sends to u_2 the information of the optimal boundary demand flow for the subsystem x^2. This demand corresponds to the optimal decision of the u_1 and is denoted by $\bar{D}_2^*$. Similarly, u_6 optimizes J_6 with respect to the boundary supply $\bar{S}$ and sends to u_5 the information of the corresponding optimal supply flow $\bar{S}_5^*$ for the subsystem x^5.

Step 2 u_2 optimizes J_2 with respect to $\bar{D}_2^*$ and sends $\bar{D}_3^*$ to u_3.

Step 3 u_3 optimizes J_3 with respect to $\bar{D}_3^*$ and sends $\bar{D}_4^*$ to u_4.

Step 4 First u_4 guesses the optimal solution u_4^* and sends it to u_5 with the information of $\bar{D}_4^*$. Next, u_5 optimizes J_5 with respect to u_4^*, $\bar{D}_4^*$, $\bar{S}_5^*$. The optimal solution u_5^* together with $\bar{S}_5^*$ is then sent to u_4 that similarly optimizes J_4 with respect to u_5^*, $\bar{D}_4^*$, $\bar{S}_5^*$ and sends u_4^* to u_5. The procedure is terminated when u_4 and u_5 reaches the Nash equilibrium.

D. Receding horizon control scheme

In this work, the optimization will be performed by using the receding horizon control (often referred also as the model predictive control) scheme that is formulated as a finite horizon optimization to be repeated on-line. Based on the measured (or estimated) current state and the predicted evolution of the exogenous signals (in our setting the boundary conditions), the controller determines the optimal input over the control/prediction horizon. From the sequence of the optimal decisions, only the first one is applied to a system, while for the next time sample the procedure is repeated. The method is particularly useful in the traffic optimization. A precise prediction of both, the state and the boundary conditions can be made only few minutes ahead. Thus, the idea of optimization that allows on a permanent information update is naturally adopted into traffic systems.

The receding horizon control scheme in our optimization problem is executed with the following steps:

Procedure 5 *(receding horizon control)*

Step 1 At time sample k estimate the state $x(k)$ and predict the evolution of the boundary conditions $\bar{D}$, $\bar{S}$, $\{\hat{D}_j\}$ in the time period $[k, k+T]$.

Step 2 Solve the Problem 1 in a distributed manner over the time period $[k, k+T]$.

Step 3 Apply the optimal decision $u^*(k)$.

Step 4 Increment time sample $k = k+1$ and continue with the Step 1.

VI. Local optimal control problem

In this section, we provide a solution for the Nash optimization problem as formulated in the section V. Namely, we will focus of the following problems: Find $u_j^* = \operatorname{argmin} J_j$ that appear in the Procedures 1–3 (the problem of finding $u_{j+1}^* = \operatorname{argmin} J_{j+1}$ in the mixed state case is treated analogously).

A. Control objectives

As stated in the introduction, our primal objective is to balance vehicle density. Since we use a non-cooperative game formulation, the balancing will be performed at the level of individual subsystems (freeway links). We will not utilize any predefined reference values. Instead, we will require that the resulting balanced density reduces travelling time acquired by the drivers associated to a subsystem. Therefore, for the local objective functions we will weight two metrics that correspond to the density balancing and the travelling time.

Let us introduce the Laplacian matrix associated to the subsystem x_j:

$$\mathrm{Lap}_j(i,\bar{i}) = \begin{cases} n_j - 1 & \text{if } i = \bar{i}\,, \\ -1 & \text{otherwise}\,. \end{cases} \tag{29}$$

For the assumed structure of the state vector $x^j = \left[\rho_1^j, \rho_2^j, ..., \rho_{n_j}^j, l_j\right]^\intercal$, the total dispersion of the vehicle density over the time interval $[0,T]$ can be measured by the following metric:

$$\begin{aligned} ||x^j||_{Lap} = &\sum_{k=0}^{T} \sum_{i \neq \bar{i}} (\rho_i^j(k) - \rho_{\bar{i}}^j(k))^2 = \\ &\sum_{k=0}^{T} (x^j(k))^\intercal \begin{bmatrix} \mathrm{Lap}_j & 0 \\ 0 & 0 \end{bmatrix} x^j(k)\,. \end{aligned} \tag{30}$$

The travelling time in freeway traffic is commonly computed by using the Total Travel Spent (TTS) metric defined as follows:

$$TTS = \Delta t \sum_{k=0}^{T} \left(\sum_{i=1}^{n_j} \rho_i^j(k) L_i^j + l_j(k) \right). \tag{31}$$

The goal in minimizing TTS is to reduce the number of vehicles in both, the mainstream and in the queues. Reduced number of vehicles in the mainstream results in increased travel velocity, and thus shortened travelling time. Reduced number of vehicles in the queue directly results in shortened queuing time. Note that TTS is a trade-off. Decreased queue

lengths increase the mainstream density and vice versa. For the sake of the adopted solution method, discussed below, we will use the quadratic objective function. By using the cell lengths matrix $L^j = \text{diag}\,(L_1^j, L_2^j, ..., L_{n_j}^j)$ the quadratic function corresponding to TTS can be written in the following form:

$$||x^j||_{TTS} = \frac{\Delta t}{2}\sum_{k=0}^{T}\left((x^j(k))^\intercal \begin{bmatrix}(L^j)^2 & 0\\ 0 & 0\end{bmatrix} x^j(k) + l_j^2(k)\right) = \frac{\Delta t}{2}\sum_{k=0}^{T}(x^j(k))^\intercal \begin{bmatrix}(L^j)^2 & 0\\ 0 & 1\end{bmatrix} x^j(k)\,. \tag{32}$$

Finally, by introducing a weighting number γ_1, we can pose the local optimal control problem, where the goal is to minimize the weighted sum of the metrics (30) and (32):

Problem 2 *(local optimal control problem)*

Find $u_j^* = \text{argmin}\, J_j$

$$J_j = \frac{\Delta t}{2}\sum_{k=0}^{T}(x^j(k))^\intercal \begin{bmatrix}\text{Lap}_j + \gamma_1\,(L^j)^2 & 0\\ 0 & \gamma_1\end{bmatrix} x^j(k)$$

Subject to $(15), (16), (10)$ for the free flow state link
$(18), (19), (10)$ for the congested state link
$(21), (22), (10)$ for the mixed state link.

Note that in the case of the mixed state links, each of the controllers tends to optimize only its controllable section, i.e. for the link $x^{j,j+1}$, u_j minimizes $J_j(x^j)$ and u_{j+1} minimizes $J_j(x^{j+1})$.

The receding horizon scheme (Procedure 5) requires solving of the Problem 1 at each time step which in practice is assumed to be less than 15 seconds. During this time, the Procedures 1–3 may demand for the solution of the Problem 2 up to several dozen times, depending on the freeway length and number of the mixed state links. Therefore, the algorithm for solving a single Problem 2 has to enable us to terminate the computation in less than 0.1 of a second. This fact supports the idea of quadratic formulation of the Problem 2. Regarding the size of our problem, the most efficient quadratic programming (QP) solvers enable to find a solution within few milliseconds (for detailed study see, for example, [18]). This time may vary depending on the initial values and the termination condition. In some cases, due to limited time, it might be necessary to terminate the computation before the optimal solution is found. In this work, instead of adopting QP solvers, we will present a solution method based on the finite horizon Linear Quadratic Regulator (LQR). To solve LQR problem, only the backward integration of the Riccati difference equation needs to be performed. Regarding the size of our problem, the computational time required for such a procedure can be neglected.

B. Internal model of the boundary flows

In order to reformulate the Problem 2 as LQR problem, at first we will transform the dynamical equations (15), (18), (21) into autonomous form (with the right hand side independent explicitly on time). For that purpose, we will utilize a simple autoregressive (AR) model that allows to build up a linear dynamical representation of the evolution of the boundary and the interfacing flows:

$$\bar{D}\,,\ \bar{S}\,,\ \{\hat{D}_j\}\,,\ \{\bar{D}_j\}\,,\ \{\hat{S}_j\}\,. \tag{33}$$

By using this representation and an extended state vector, the governing equations will take a required autonomous form.

Let us consider the following AR model:

$$z(k+1) = \sum_{i=1}^{\bar{n}} \alpha_i\, z(k+1-i)\,, \quad k = 0, 1, ...\,, \tag{34}$$

where the initial values $z(0)$, $z(-1)$,..., $z(1-\bar{n})$ are assumed to be given as current and past measurements and the set α is estimated mostly based in historical data. By evaluating the AR model, we obtain a short-term forecasting. In our setting, we consider reverse problem. We assume that at each time instant the prediction of the boundary flows are given over the time horizon T. By using this information and the the set of initial values, we calibrate AR models by using the method of least squares. The prediction of the boundary flows $\bar{D}$, $\bar{S}$, $\{\hat{D}_j\}$ may be obtained by using, for instance, non-parametric regression or neural network based methods. The interfacing flows $\{\bar{D}_j\}$, $\{\bar{S}_j\}$ are evaluated by using the dynamical equations (15), (18) and (21).

In order to represent AR model in the standard dynamical form of $z(k+1) = f(z(k))$, we introduce the following state vector:

$$z = [z_1, z_2, ..., z_{\bar{n}}]^\intercal \tag{35}$$

defined as: $z_1(k) = z(k)$, $z_2(k) = z(k-1)$,..., $z_{\bar{n}}(k) = z(k+1-\bar{n})$. Then, by introducing:

$$A_z = \frac{1}{\Delta t}\begin{bmatrix}1-\alpha_1 & \alpha_2 & \cdots & \alpha_{\bar{n}}\\ 1 & -1 & & \\ & \ddots & \ddots & \\ & & 1 & -1\end{bmatrix} \tag{36}$$

(34) can be written as follows:

$$z(k+1) = z(k) + \Delta t\, A_z\, z(k)\,. \tag{37}$$

with the initial condition: $z_1(0) = z(0)$, $z_2(0) = z(-1)$,..., $z_{\bar{n}}(0) = z(1-\bar{n})$. The form of (37) will now enable us to merge the flows into the dynamics of our local systems. Let us first consider the free flow state link. We introduce AR model vectors $z^{\bar{D}_j}$, $z^{\hat{D}_j}$ representing $\bar{D}_j$ and $\hat{D}_j$, respectively. The extended state vector of the free flow state link will be defined as:

$$y^j = \left[x^j, z^{\bar{D}_j}, z^{\hat{D}_j}\right]^\intercal\,. \tag{38}$$

The dynamical equation of the free flow state link (15) is represented as follows:

$$y^j(k+1) = y^j(k) + \Delta t\,\left(\bar{A}_f y^j(k) + \bar{B}_f u_j(k)\right)\,. \tag{39}$$

Here $\bar{A}_f$ has a block diagonal structure composed of A_f and two matrices A_z. The vector $\bar{B}_f$ is build upon B_f. Similarly, by introducing:

$$y^j = \left[x^j, z^{\bar{S}_j}, z^{\hat{D}_j}\right]^\intercal\,, \tag{40}$$

where now $z^{\bar{S}_j}$ refers to $\bar{S}_j$, we can represent the governing equations for the congested state link (18):

$$y^j(k+1) = y^j(k) + \Delta t \, \left(\bar{A}_c y^j(k) + \bar{B}_c u_j(k)\right) . \quad (41)$$

In the case of the mixed state link, we introduce the extended state vector as:

$$y^{j,\,j+1} = \left[x^{j,\,j+1}, z^{\bar{D}_j}, z^{\hat{D}_j}, z^{\bar{S}_{j+1}}, z^{\hat{D}_{j+1}}\right]^\intercal , \quad (42)$$

where $z^{\bar{D}_j}$, $z^{\hat{D}_j}$, $z^{\bar{S}_{j+1}}$ and $z^{\hat{D}_{j+1}}$ corresponds to $\bar{D}_j$, $\hat{D}_j$, $\bar{S}_{j+1}$ and $\hat{D}_{j+1}$, respectively. The dynamics (21) is now represented by:

$$\begin{aligned} y^{j,\,j+1}(k+1) &= y^{j,\,j+1}(k) + \Delta t \, \bar{A}_{fc}(k) y^{j,\,j+1}(k) + \\ &+ \Delta t \left(\bar{B}_f u_j(k) + \bar{B}_c u_{j+1}(k)\right) . \end{aligned} \quad (43)$$

A practical advantage arising from the use of AR model is that of significantly reduced amount of data needed to be exchanged by the controllers during the optimization process. The full information of the interfacing flows $\{\bar{D}_j\}$ and $\{\bar{S}_j\}$ is now stored within the set of parameters $\{\alpha_i\}$. In practice, it is sufficient to use 4–5 parameters to represent flow time series of 30-50 values.

C. LQR problem

Having the autonomous representation of the dynamical equations we are ready to reformulate the Problem 2 into LQR problem. Let us first introduce the matrix:

$$Q = \mathrm{diag}(\mathrm{Lap}_j + \gamma_1 \, (L^j)^2, \gamma_1, 0) . \quad (44)$$

Here, for the extended state vector y^j, the sub-matrix $\mathrm{Lap}_j + \gamma_1 \, (L^j)^2$ and the scalar γ_1 will correspond to the state vector x^j, while 0 will refer to uncontrollable states $z^{\bar{D}_j}$, $z^{\hat{D}_j}$, ($z^{\bar{S}_{j+1}}$, $z^{\hat{D}_{j+1}}$). Consider then the problem:

Problem 3 *(local LQR problem)*

Find $u_j^* = \mathrm{argmin}\, J_j$

$$J_j = \frac{\Delta t}{2} \sum_{k=0}^{T} \left((y^j(k))^\intercal \, Q \; y^j(k) + \gamma_2 (u_j(k))^2\right)$$

Subject to (39) in the case of the free flow state link
(41) in the case of the congested state link
(43) in the case of the mixed state link .

Note that Q is positive semi-definite. To assure the convexity of the problem, we introduced the strictly positive term with the weighting number γ_2. The reader can easily observe that the Problems 2 and 3 are equivalent, except for the set of constraints (16), (19), (22), (10) that were omitted in LQR formulation. In the implementation, the solution to the Problem 3 will be saturated with the bounds determined by these constraints. By using the necessary optimality condition, the solution to the Problem 3 is as follows:

$$u_j^*(k) = -\frac{1}{\gamma_2} \bar{B}^\intercal \, K(k) \, y^j(k) , \quad (45)$$

where $K(k)$ is the solution to the Riccati difference equation:

$$\begin{aligned} &\frac{1}{\Delta t}(K(k+1) - K(k)) = K(k)\bar{A} + \bar{A}^\intercal K(k) + \\ &- \frac{1}{\gamma_2} K(k) \bar{B} \bar{B}^\intercal K(k) + Q , \; K(T) = 0 . \end{aligned} \quad (46)$$

In (45) and (46), depending on the state of the link, the appropriate matrices for $\bar{A}$ (i.e. $\bar{A}_f$ or $\bar{A}_c$ or $\bar{A}_{fc}$) and $\bar{B}$ (i.e. $\bar{B}_f$ or $\bar{B}_c$ or $\bar{B}'_f$ ($\bar{B}'_c$)) are supposed to be inserted. In the case of the mixed state link, it is assumed that the matrix $\bar{A}_{fc}$ is constant over the time period $[0, T]$.

VII. Study Cases

The developed control method will be tested on the CTM model of the south ring of Grenoble – a two lane highway that connects the city of Grenoble in the north-east to south-west linking the highways A41 and A480. At the present moment, the ring is equipped with data collection system based on magnetic sensors. Ramp metering technology is planned to be installed by the end of 2014. For the optimization, we chose

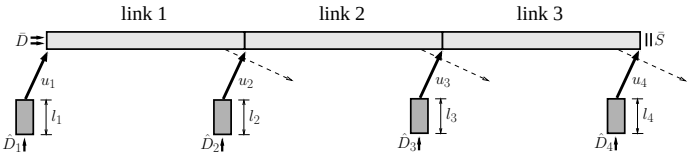

Figure 12. A three link section of the south ring of Grenoble used in the simulations.

the western section of the ring of the length 6.07 [km]. On the considered direction, i.e. from east to west, this section is equipped with 4 on-ramps and 3 off-ramps (all of them are one lane) as demonstrated in Fig. 12. The estimated model parameters are summarized in the table I. For the split ratios we assume $\bar{\beta}_1 = 0.82$, $\bar{\beta}_2 = 0.80$, $\bar{\beta}_2 = 0.80$. The merging parameters $p = 0.3$ are assumed to be identical for each of the links.

Table I
The Cell-Transmission Model parameters used in the simulations.

	v [km/h]	w [km/h]	$\bar{\rho}$ [veh/km]	link length [km]
link 1	82	20	280	1.57
link 2	78	21	280	1.66
link 3	80	20	280	2.84

In this study, we will consider two scenarios: one for uniformly congested traffic, and the other for transient traffic. In the first case, be means of previously defined metrics, we will examine the performance of the control method under steady congested boundary conditions. In the second case, we will begin the simulation of the free flow traffic with drop of downstream capacity. The goal will be to investigate the impact of state balancing on the propagation of the shock wave. Both cases will be evaluated with the time step of 5 seconds. We assume 20 time steps for the control/prediction horizon in the receding horizon scheme. Control decision will

be updated every time step. We will demonstrate the results through a comparison of the optimal solutions (referred as closed-loop) with the evolution of the open-loop system, i.e. when the on-ramp demand stays uncontrolled.

A. Uniformly congested traffic

In this case, the initial values for density were randomly selected from the interval $[170, 210]$ [veh/km]. The initial queue lengths were set to $l_j = 10$ [veh] for all j. In accordance to the information pattern introduced in the section IV, the controllers u_2, u_3 and u_4 under the congested state will optimize the links 1, 2 and 3, respectively. The simulations will be carried over the time interval of 20 minutes under the following steady boundary conditions: $\bar{S} = 3100$ [veh/h], $\hat{D}_j = 800$ [veh/h] for all j. The state plots will be given only for the link 1. Trajectories for the other links do not exhibit any qualitative differences. Each of the links was split into 5 cells of the same length.

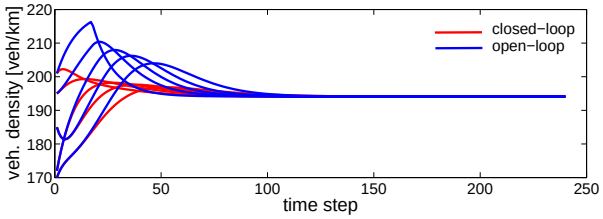

Figure 13. Evolution of the mainstream state in the link 1 (each of the curves represent one cell).

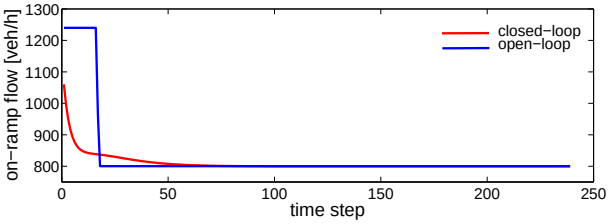

Figure 14. Comparison of the on-ramp flows in the entrance 2.

The on-ramp flow in the entrance 2 and the corresponding evolutions of the vehicle densities in the link 1 are depicted in Figs. 14 and 13, respectively. We can observe that the closed-loop system rapidly converges to a common value. To demonstrate better the convergence rate, Fig. 15 compares the evolutions of the balancing metric defined as:

$$||x^j||_{Lap}(k) = (x^j(k))^\intercal \begin{bmatrix} \mathrm{Lap}_j & 0 \\ 0 & 0 \end{bmatrix} x^j(k)\,. \qquad (47)$$

The comparison of the balancing metric $||x^j||_{Lap}$ (as defined in (30)) is presented in the table II. Each value represents the metric computed in the closed-loop case divided by the metric in the case of open-loop system. For each of the links, the balancing metric was decreased more than 40 percent.

From Fig. 13, we can observe that the closed loop system keeps lower mainstream density values which has a positive

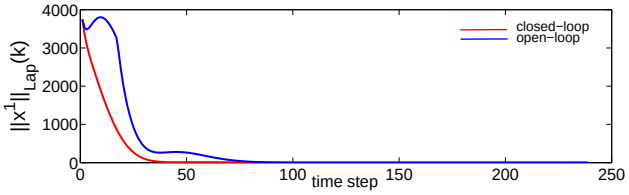

Figure 15. Evolution of the balancing metric for the link 1. The closed-loop system evidently improves the convergence rate.

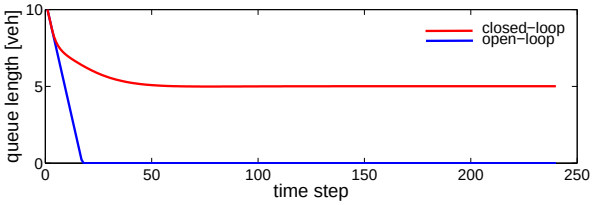

Figure 16. Evolution of the queue length in the entrance 2.

impact on the travelling time. However, to justify the Total Travel Time, we need to check also the states in the queues. The controlled on-ramp flow (see Fig. 14) is lower than in the open-loop case, and thus the queue is being released slower as depicted in Fig. 16. As a result, in the steady state, there is still 4 vehicles queuing. Nevertheless, the overall travelling time computed by the norm $||x^j||_{TTS}$ (as defined in (32)) is decreased by 2–3 percent for each of the links. The weighted sum of the balancing and the travelling time metrics was reduced by 7–8 percent.

Table II
METRIC COMPARISON. EACH VALUE REPRESENTS THE QUOTIENT: (METRIC FOR CLOSED-LOOP CASE)/(METRIC FOR OPEN-LOOP CASE).

	$\|\|x^j\|\|_{Lap}$	$\|\|x^j\|\|_{TTS}$	$\|\|x^j\|\|_{Lap} + \gamma_1\|\|x^j\|\|_{TTS}$
link 1	0.58	0.97	0.92
link 2	0.56	0.98	0.93
link 3	0.45	0.98	0.92

B. Transient traffic

Transient traffic refers to the situations in which we observe the congestion either expanding or contracting. In particular, we can encounter the shock waves caused by the instantaneous drops of capacity. To test the designed control method under the presence of shock wave, we consider the following scenario. We initialize the simulation with some free flow state and on-ramp boundary flows $\hat{D}_j = 600$ [veh/h] for all j. For the first 150 time steps we reproduce the capacity drop by setting $\bar{S} = 2800$ [veh/h]. During this time, we will observe a shock wave propagating upstream. For the time steps 151-400, we will set $\bar{S} = 3800$ [veh/h] that will bring the system back to the free flow state. In this setting, the controller 1 will optimize the free flow section 1 by solving the hierarchical game. The other controllers will be involved into both, the hierarchical and the competitive games, since the sections 2 and 3 will be

under the mixed states. To better capture the movement of the congestion wave, we divided each of the links into 8 cells.

The evolution of density over the considered freeway length can be represented by colormaps as depicted in Fig 17 (open-loop case) and Fig 18 (closed-loop case). The green color indicates the free flow state ($\rho^{cr} = 56$ [veh/km]). The bottleneck, located at the right boundary, caused the shock wave propagating upstream. The shock speed corresponds to the slope of the congestion front (see the blue angle in Fig 18). Lower the slope then faster the shock wave propagation. For comparison, in Fig 18 we marked the open-loop profile with the dashed line. We can observe that in the closed-loop case, the congestion propagates slower, and as a result, it expands approximately 500 meters shorter than in the open-loop case. Note also that during the first 150 time steps for the closed-loop system, the density in the link 3 keeps lower value.

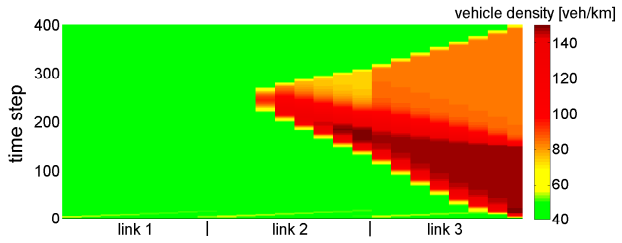

Figure 17. Space-time distribution of vehicle density in the case of open-loop system. The green area corresponds to the free flow state.

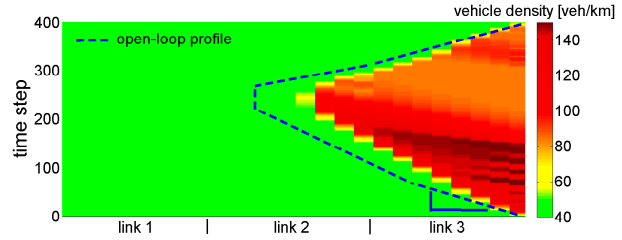

Figure 18. Space-time distribution of vehicle density in the case of closed-loop system. Dashed line stands for the open-loop profile. Indicated slope corresponds to the shock wave speed (lower the slope–higher the speed).

VIII. Conclusion

In this paper, we have presented a method for distributed optimal balancing of vehicle distribution over freeway via use of ramp meters. In this method, the controllability has been taken as the principle underlying both, the system partitioning and the topology of the information exchange. As we have demonstrated, the selection of the controllable subsystems strictly depends on the traffic state. This fact is often ignored in the methods of freeway traffic optimization while the controllability is a crucial factor in the convergence of numerical procedures. To execute the optimization under the assumed information patterns, we have formulated a non-cooperative Nash problem. It follows that this formulation is not only convenient for a design of distributed optimization scheme process, but, under the defined balancing objective, it may also cause the slow down of the congestion propagation. For the future works, the authors are planning to validate the method on the real freeway system with a comparison to existing control strategies.

References

[1] G. Gomes, R. Horowitz, Optimal Freeway Ramp Metering Using the Asymmetric Cell Transmission Model, *Transportation Research Part C*, vol. 14, 2006, pp 244-262.

[2] Y. Li, E. Canepa, Ch. Claudel, Optimal Control of Scalar Conservation Laws Using Linear/Quadratic Programming: Application to Transportation Networks, *Control of Network Systems*, vol. 1, 2014, pp 28-39.

[3] A. Hegyi, B. De Schutter, J. Hellendroon, T. van den Boom, Optimal Coordination of Ramp Metering and Variable Speed Control – An MPC Approach, *IEEE American Control Conference*, 2002, pp 3600-3605.

[4] D. Jacquet, C. Canudas-de-Wit, D. Koenig, Optimal Control of Systems of Conservation Laws and Application to Non-Equilibrium Traffic Control, *Proceedings of the 13th IFAC Workshop on Control Applications of Optimisation*, 2006.

[5] D. Sun, A. Clinet, A.M. Bayen, A Dual Decomposition Method For Sector Capacity Constrained Traffic Flow Optimization, *Transportation Research Part B*, 2011, pp 880-902.

[6] A. Ferrara, A. Nai Oleari, S. Sacone, S. Siri, Freeway Networks as Systems of Systems: an Event-Triggered Distributed Control Scheme, *IEEE International Conference on System of Systems Engineering*, 2012, pp 197-202.

[7] J. R. D. Frejo, E. F. Camacho, Global Versus Local MPC Algorithms in Freeway Traffic Control with Ramp Metering and Variable Speed Limits, *IEEE Transaction on Intelligent Transportation Systems*, vol 13, 2012, pp 1556-1565.

[8] C. Portilla, F. Valencia, J.D. Lopez, J. Espinosa, A. Nunez, B. De Schutter, Non-linear Model Predictive Control Based on Game Theory for Traffic Control on Highways, *Proceedings of the 4th IFAC Nonlinear Model Predictive Control Conference*, 2012, pp. 436-441.

[9] L. Giovanini, J. Balderud, Game Approach to Distributed Model Predictive Control, *International Control Conference*, 2006.

[10] D. Pisarski, C. Canudas-de-Wit, Analysis and Design of Equilibrium Points for the Cell-Transmission Traffic Model, *IEEE American Control Conference*, 2012, pp 5763-5768.

[11] D. Pisarski, C. Canudas-de-Wit, Optimal Balancing of Road Traffic Density Distributions for the Cell Transmission Model, *IEEE Conference on Decision and Control*, 2012, pp 6969-6974.

[12] C. Daganzo, The Cell Transmission Model, A Dynamic Representation of Highway Traffic Consistent with the Hydrodynamic Theory, *Transportation Research Part B*, vol. 28, 1994, pp 269-287.

[13] S. K. Godunov, A Difference Scheme for Numerical Solution of Discontinuous Solution of Hydrodynamic Equations, *Math. Sbornik*, vol 47, 1969.

[14] R. J. LeVeque, *Numerical Methods for Conservation Laws*, Birkhauser Verlag, Basel; 1992.

[15] C. Daganzo, The Cell Transmission Model: Part II: Network Traffic, *Transportation Research Part B*, vol. 29, 1995, pp 79-93.

[16] H. Zhang, S. G. Ritchie, W. W. Recker, Some General Results on the Optimal Ramp Metering Control Problem, *Transportation Research Part C*, vol. 4, 1996, pp 51-69.

[17] T. Basar, G. J. Olsder, *Dynamic Noncooperative Game Theory*, SIAM Classics edition, 1999.

[18] Y. Wang, S. Boyd, Fast Model Predictive Control Using Online Optimization, *IEEE Transactions on Control Systems Technology*, vol 18, 2010, pp 267-278.

[19] E. I. Vlahogianni, J. C. Golias, M. G. Karlaftis, Short-term Traffic Forecasting: Overview of Objectives and Methods, *Transport Reviews*, vol 24, 2004, pp 533-557.